ChemComm

Accepted Manuscript

This is an *Accepted Manuscript*, which has been through the Royal Society of Chemistry peer review process and has been accepted for publication.

Accepted Manuscripts are published online shortly after acceptance, before technical editing, formatting and proof reading. Using this free service, authors can make their results available to the community, in citable form, before we publish the edited article. We will replace this *Accepted Manuscript* with the edited and formatted *Advance Article* as soon as it is available.

You can find more information about *Accepted Manuscripts* in the **Information for Authors**.

Please note that technical editing may introduce minor changes to the text and/or graphics, which may alter content. The journal's standard **Terms & Conditions** and the **Ethical guidelines** still apply. In no event shall the Royal Society of Chemistry be held responsible for any errors or omissions in this *Accepted Manuscript* or any consequences arising from the use of any information it contains.

Journal Name

COMMUNICATION

Amide and N-oxide functionalization of T-shaped ligand for isoreticular MOFs with giant enhancement in CO$_2$ separation

Ying Xiong,[a] Yuan-Zhong Fan,[a] Rui Yang,[a] Sha Chen,[a] Mei Pan,[a] Ji-Jun Jiang,*[a] and Cheng-Yong Su*[ab]

By stepwise functionalization of a T-shaped ligand with amide and N-oxide groups, we obtained isoreticular MOFs with drastically strengthened CO$_2$–framework interactions induced by newly proposed "open donor sites" (ODSs) effect, resulting in high heat of adsorption and CO$_2$/CH$_4$, CO$_2$/CO and CO$_2$/N$_2$ separation selectivities at room temperature.

The CO$_2$ capture and separation (CCS) process has caught public attentions and is under urgent investigation in laboratories all over the world due to industry demand and imminent circumstance of global climate change.[1] Nowadays industry scale of CCS mostly uses amine solvents as CO$_2$ capture adsorbents,[2] which suffers from high cost of regeneration, excessive corrosion and toxicity issues.[3] In past decade, newly emerged porous materials[4] like metal-organic frameworks (MOFs) have attracted great attention owing to their tailorable porosity, moderate affinity toward CO$_2$ and suitable adsorption kinetics, and a great of efforts have been devoted to their potential applications in gas storage, separation,[5] as well as catalyst.[6]

In order to develop MOFs for efficient CO$_2$ separation, some effective strategies have been applied. For example, modification of the pore surface by introducing functional groups, such as –CH$_3$, –NO$_2$, –NH$_2$, –OH, –COOH,[7] or exposed N sites,[8] has been proven to be able to tune the polarity and acidity of porous environment, thus offer higher affinity towards CO$_2$ to boom adsorption amount and selectivity. Another successful approach to promote CCS of MOFs is to create so-called "open metal sites" (OMS, or coordinatively unsaturated sites, CUS) usually produced by removal of weakly coordinating solvents.[9] Specific interactions between the electron-rich orbital of adsorbate and vacant orbital of OMS increase CO$_2$ adsorption capacity of MOFs. However, remove of coordinating solvents in many occasions would result in decomposition of the whole framework, or, the metal site might transform its coordination geometry to a thermodynamically more stable form instead of keeping the metal site open.[10] Other effective methods include the use of flexible MOFs as well as MOFs with specific narrow pores.[11]

Herein, we propose an alternative way to combine both contributions from bridging ligand and coordination sites. As shown in Fig. 1, we first prepare a T-shaped functional ligand[12] to incorporate amide group into the ligand bridge (H$_2$INIA: 5-(isonicotinoylamino)isophthalic acid). Furthermore, we introduce N-oxide group as charge variable coordination site (H$_2$INOIA: 5-

(isonicotinoylamino N-oxide)isophthalic acid). The pyridyl N-oxide has been known as an intriguing unit for generation of MOFs[13] with magnetism[14] and fluorescence.[15] However, the adsorption property endowed by this group have not been well studied,[16] and its effect towards CO$_2$ uptake has not been understood. Compared to the common pyridine-N donor, the N-oxide donor can bring charge-separated character and metal-binding variation to the coordination site. As seen from Fig. 1 and S1, the resulting O donor has two long pair electrons, which can bind one metal in a bent fashion with ∠M-O-N angle of *ca.* 120° and leave another lone pair electrons to interact with electrophilic atom of guest. Such unique charge-separated character plus electron-rich bent coordination of N-oxide donor may provide enhanced affinity towards CO$_2$ to match its distinct electrophilicity of C and O atoms (Fig. S1). Therefore, the N-oxide donor might offer an alternative type of coordination site to capture CO$_2$, denoted here as "open donor sites" (ODSs), in comparison to the well-known OMS or CUS.
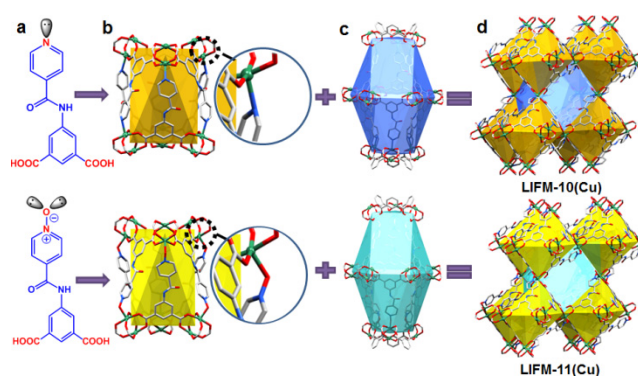

Fig. 1 (a) Ligands **H$_2$INIA** and **H$_2$INOIA** showing donor character. (b,c) 6- and 12-nuclear Cu-cages and coordination environments. (d) 3D ScD$_{0.33}$ Framework. Color mode: green, Cu; gray, C; blue, N; red, O. H atoms are omitted.

The structural model of MOFs based on the T-shaped ligand and paddlewheel units have been previously reported by us and others and fully rationalized by Eddaoudi *et al.*[11] as an effective MOF pillaring strategy. Through a ligand-to-axial approach[11e] 3D MOFs of rtl or ScD$_{0.33}$ topologies could be generated based on pillaring of the 2D edge transitive nets, sql and kgm, respectively. This gives us a chance to construct isoreticular MOFs by using T-shaped ligands

H$_2$INIA and H$_2$INOIA which have the similar coordination behavior but slightly varied bridging length (Fig. 1).

As expected, solvothermal reactions of Cu^{2+} with H$_2$INIA and H$_2$INOIA afforded two isoreticular MOFs LIFM-10 and LIFM-11 (LIFM: Lehn Institute of Functional Materials), respectively. Single-crystal analyses verified their isostructures with the asymmetric unit containing one Cu^{2+} ion and one T-shaped ligand (Figs. 1, S1-2 and Table S1-2). Typically, every two Cu^{2+} ions are chelated by four carboxylate groups from four different ligands to form classical secondary building unit of square paddle-wheel Cu$_2$(O$_2$CR)$_4$ cluster. The axial positions of the Cu$_2$(O$_2$CR)$_4$ cluster are satisfied by two pyridine-N (LIFM-10) or N-oxide O (LIFM-11) donors from other two ligands. Therefore, the whole coordination skeleton can be regarded as a 3D framework based on 2D kgm sheets constituted of 4-connected Cu$_2$(O$_2$CR)$_4$ clusters and pillars provided by isonicotinoylamino or isonicotinoylamino N-oxide bridges. The T-shaped ligands serve as 3-connected nodes while the paddlewheel clusters as 6-connected nodes, thus generating a (3,6)-connected framework of ScD$_{0.33}$ topology as calculated by Topos 4.0.[17]

One unique structural feature in these two isoreticular frameworks is that the axial coordination of Cu^{2+} from pyridine-N donor or N-oxide donor is in bent fashion as seen from Fig. 1a. In LIFM-10 the pyridyl plane shows a tensely bent angle of 152.5° with regard to N-Cu bond; while in LIFM-11, the ∠N-O-Cu angle of 119.1° is natural due to metal-ligand bonding via one long pair electrons of sp^2 O donor, which is important for CO$_2$ interactions (*vide infra*). Furthermore, two types of cavities are formed: one is 6-nuclear Cu-cage and the other 12-nuclear Cu-cage (Fig. 1, diameters: 8 and 12 Å in LIFM-10; 9 and 12 Å in LIFM-11). These cages are aligned alternately in parallel to constitute 1D hourglass-shaped channels (Fig. S2), which afford considerable void spaces (59% in LIFM-10 and 60% in LIFM-11 calculated by PLATON[18]) for gas uptake.

Thermal stability of the coordination frameworks was testified by TGA analyses, which unveiled that a larger amount of solvents could be removed by heating, and the frameworks started to decompose at about 270 °C (Fig. S4-5). The framework robustness was confirmed by variable temperature powder X-ray diffraction (VT-PXRD) to be able to maintain the permanent porosity up to 260 °C (Figs. S6-7). Therefore, activation of the porous frameworks was simply carried out by heating in vacuum at 150 °C. As seen from Figs. S8-9, the activated samples gave broaden peaks on PXRD patterns, indicating degradation of crystallinity but persistence of framework porosity. The crystal samples are stable in air, however, slight framework changes can be observed by XRD monitoring of samples when immersed in water (Figs. S28-29).

The N$_2$ sorption measurements for LIFM-10 and LIFM-11 at 77 K both show typical type-I adsorption isotherms (Fig. S10), evidently indicative of microporous gas uptake behaviors. Table 1 lists the experimental and simulated results of BET surface areas and total specific pore volumes for two MOFs. It is noted that the experimental BET areas of two MOFs are slightly lower than the simulated ones, suggesting little collapsing/blocking of pores during activation, especially for LIFM-11, which is in accordance with the PXRD observation (Fig. S9). However, the final total pore volumes reach to comparable values after N$_2$ uptake.
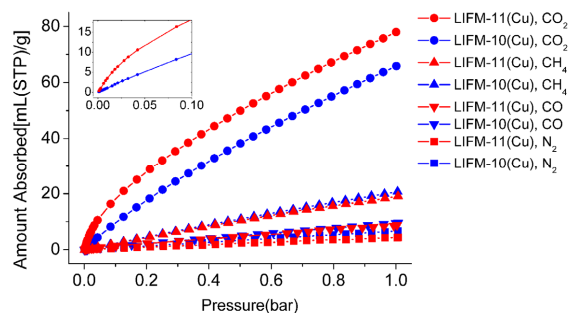

Fig. 2 Gas adsorption isotherms at 298 K. Red: **LIFM-11**; Blue: **LIFM10**. Inset: enlarged CO$_2$ adsorption isotherms of **LIFM-10** and **LIFM-11** below 0.1 bar.

Permanent porosity of two MOFs established by N$_2$ sorption promotes us to detect their CO$_2$ uptake capacities and selectivities at room temperature. As shown in Fig. S11-12, adsorption isotherms disclose they exhibit almost the same high CO$_2$ uptake capacity at 1 atm and 273 K: 129.5 mL/g (20.3%wt) for LIFM-10 and 129.6 mL/g (20.3%wt) for LIFM-11. However, as the temperature arises, CO$_2$ storage capacity of LIFM-11 surpasses that of LIFM-10 (65.9 mL/g vs 78.0 mL/g at 298 K). After carefully examining their CO$_2$ adsorption behaviors, it turns out that LIFM-11 performs better because of a more abrupt rise at relatively low pressures (~ 0.1 atm, Fig. 2 inset). This obvious enhancement could be mainly attributed to the optimized interactions between CO$_2$ and the pore surface, which hints at existence of effective affinity adsorption sites contributed by N-oxide groups in LIFM-11 (*vide infra*).[19]
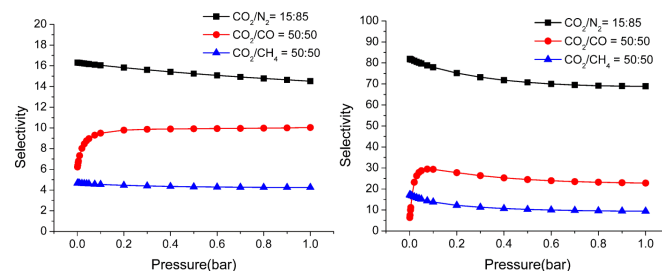

Fig. 3 Selectivities of CO$_2$ versus CH$_4$, N$_2$ and CO calculated from IAST based method. Upper: **LIFM-10**; Lower: of **LIFM-11**.

On the basis of CO$_2$, CH$_4$, CO and N$_2$ isotherms measured at 298 K (Fig. 2), the separation selectivities of CO$_2$ versus CH$_4$, N$_2$ and CO were calculated up to 1 atm from ideal adsorption solution theory (IAST) based method (Fig. 3, Table 1, see SI),[20] which predicts separation performance for 15/85:CO$_2$/N$_2$, 50/50:CO$_2$/CH$_4$ and 50/50:CO$_2$/CO binary mixtures mimicking those in natural gas upgrading, post-combustion capture and biogas purification processes. In general, the IAST selectivities of CO$_2$/CH$_4$ and CO$_2$/N$_2$ are slightly decreased as the pressure increases. Surprisingly, the CO$_2$/CO selectivity shows a rapid increase from the starting point at low pressure (~ 0.1 atm). This means CO may have unordinary uptake behavior at the very beginning. If only considering the starting values calculated by IAST method, all IAST selectivities are closely comparable with those obtained by the Virial based method (Table 1, S4-5, Figs. S13-22) which are usually calculated for the

Table 1. Pore textural property and separation selectivity^a

Sample	Experimental			Simulation		Initial enthalpy	IAST Selectivity ^{e}			Virial Selectivity		
	S_{BET} (m^2/g) ^{b}	V_t (cc/g)^{ca}	D (Å) ^{d}	S_{BET} (m^2/g)	V_t (cc/g)	Q_{st} (kJ/mol)	CO$_2$/CH$_4$	CO$_2$/CO	CO$_2$/N$_2$	CO$_2$/CH$_4$	CO$_2$/CO	CO$_2$/N$_2$
LIFM-10(Cu)	1550	0.64	6 × 6	1791	0.66	29	4.7~4.3	6.2~10.0	16.3~14.5	5.0	5.8	18.3
LIFM-11(Cu)	1176	0.68	5 × 5	1695	0.66	53	17.2~9.4	6.4~22.8	81.9~68.9	17.4	5.2	64.4

^{a} Data at 298 K. ^{b} BET surface area. ^{c} Total pore volume. ^{d} Effective pore size. ^{e} CO$_2$/CH$_4$ = 50:50; CO$_2$/CO = 50:50; CO$_2$/N$_2$ = 15:85, 0~1 bar.

ChemComm Accepted Manuscript

zero coverage evaluations. Fig. 4 illustrates a comparison of CO_2 separation performance of LIFM-10 and LIFM-11 with some other MOFs evaluated by IAST method under similar conditions.[21] It is immediately clear that LIFM-11 shows outstanding selectivities of CO_2/CH_4 and CO_2/N_2 when compared with MOF-5, HKUST-1 and PCN-11 at room temperature and 1 atm. Meanwhile, it is noteworthy that the separation selectivities of LIFM-11 are significantly improved in contrast to LIFM-10, e.g. more than 2-fold for CO_2/CH_4 and CO_2/CO, and 5-fold for CO_2/N_2. This means that functionalization of the T-shaped ligand with N-oxide group can remarkably optimize CO_2 affinity toward pore surface. Similar enhancement of CO_2 selectivities over CH_4 and N_2 have been observed in porous MPM-1 by replacing Cl^- with TiF_6^- anions.[22a] However, it should be noted that even exceptional CO_2/CH_4 and CO_2/N_2 selectivities have been achieved by strictly limiting the pore shape and size, as well as introducing anionic interactions or chemisorbent-like behaviors,[21,22] e.g. 231 for CO_2/CH_4 and 1818 for CO_2/N_2 in SIFSIX-Zn, 590 for CO_2/N_2 in [Cu(bcpm)H$_2$O], and 182 for CO_2/N_2 in Mg-MOF-74. If taking the Virial selectivity for comparison, LIFM-11 also surpasses known MOFs like MOF-5 (15.5 for CO_2/CH_4; 17.5 for CO_2/N_2),[23a] ZIF-78 (10.6 for CO_2/CH_4; 50.1 for CO_2/N_2),[23b] en-Cu-BTTri (44 for CO_2/N_2),[23c] and widely used industrial BPL AC (activated carbon: 3.8 for CO_2/CH_4; 20 for CO_2/N_2)[24] under the same conditions, but similarly, could not reach to high values of a few MOFs possessing OMSs, exposed N sites or chemisorbed groups.[21,22,25] Finally, it is notable that LIFM-11 displays excellent CO_2/CO IAST selectivity (22.8) at 1 atm, which is very crucial in oxy-combustion process[1b] but rarely studied.
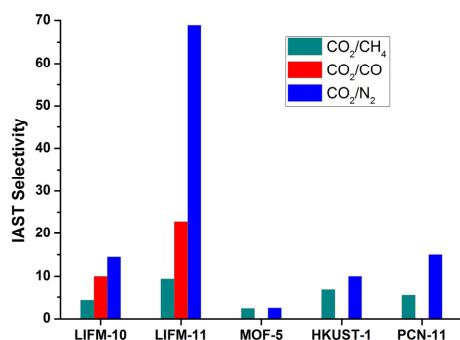

Fig. 4 Comparison of CO_2/CH_4, CO_2/CO and CO_2/N_2 selectivities of **LIFM-10** and **LIFM-11** with other MOFs checked by IAST method under similar conditions.[24]

To explore why LIFM-11 exhibits higher CO_2 separation selectivities than LIFM-10, their isosteric heats (Q_{st}) were calculated from the sorption data measured at 273, 298 and 308 K by the Virial fitting method (Figs. S13-14).[26] A significant increase (183%) of CO_2 Q_{st} value was observed for LIFM-11 in comparison to LIFM-10, giving the enthalpies at zero coverage of 53 and 29 kJ/mol (Fig. 5a, Table 1 and S3), respectively. In the case of LIFM-11, the Q_{st} values decrease steadily upon CO_2 loading, reaching to a plateau around 28 kJ/mol after 1 mmol/g uptake of CO_2. Such shape of curve is characteristic for MOFs that possess specific CO_2 adsorption sites embedded in pore walls,[25a,27] suggesting that strong CO_2–framework interactions have been introduced by N-oxide functionalization in LIFM-11. On the contrary, the curve of LIFM-10 shows a rather gently decrease during the adsorption process, indicative of much more homogenous binding sites in LIFM-10. To our knowledge, the CO_2 Q_{st} of LIFM-11 at zero loading is the highest value among MOFs containing saturated metal centers, comparable to those of top-performing MOFs possessing OMSs and exposed N sites, but lower than those having functional amines groups (Table S3).

The experimental data were treated and interpreted by simulated annealing techniques[8b,28] and periodic DFT calculations (see SI) to understand the mechanism of CO_2 adsorption and the nature of CO_2–framework interactions. Charge analysis of two MOFs revealed a significant charge variation (Fig. S23) after oxidization of pyridine-N. In LIFM-10, pyridine-N carries a negative charge of -1.118e. While in LIFM-11, O and N atoms of the N-oxide group carry opposite charges of -0.889e and 0.623e, respectively. Such charge-separate nature, together with the electron-rich and bent coordinating N-oxide donor, provide preferential CO_2 adsorbing sites on the pore surface of LIFM-11 in contrast to LIFM-10 (Figs. 1 and S24).
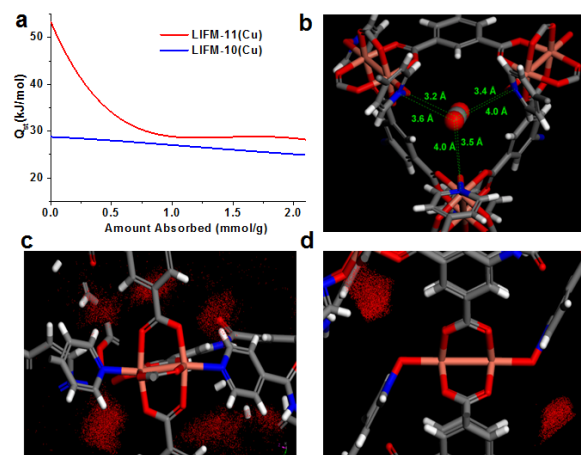

Fig. 5 (a) Calculated isosteric heats of CO_2 adsorption on **LIFM-10** and **LIFM-11**. (b) Preferred CO_2 adsorption sites by annealing simulations for **LIFM-11**. Close contact distances in Å. (c,d) Partial distribution of CO_2 adsorbed in **LIFM-10** and **LIFM-11**.

Preferred CO_2 binding sites were estimated by the annealing simulations. As illustrated in Figs. 5 and S25, the CO_2 molecules adsorbed in pores of LIFM-10 distribute broadly around the carboxylate groups and benzene rings. By contrast, CO_2 molecules in LIFM-11 pores are predominantly located right to the O donors of N-oxide groups. Figs. 5b and S26 demonstrate the mainly preferred positions of CO_2 adsorption. In LIFM-10, CO_2 molecules are widely found around the corner of paddle-wheel clusters with C in CO_2 forming close contact with carboxyl O (d_{C-O} = 3.5 Å), or around the benzene rings with O in CO_2 shortly interacting with aromatic C (d_{O-C} = 3.1 Å). On the contrary, CO_2 molecule in LIFM-11 mainly interact with three surrounding N-oxide groups (d_{C-O} = 3.2-3.5 Å; d_{N-C} = 3.6-4.0 Å). As seen in Fig. 5b, CO_2 molecule lies alongside the N-oxide groups with electron deficient C of CO_2 forming short contacts with the negatively charged O of N-oxide, and the electron rich O of CO_2 shortly contacting with the positively charged N of N-oxide. This result exactly elucidates the nature of N-oxide as a CO_2 binding ODS and the mechanism of enhanced CO_2–framework affinity in LIFM-11, leading to higher Q_{st} value and separation selectivity. These results confirm that the N-oxidation in LIFM-11 can bring new effective adsorption sites for CO_2, significantly attributing to the high CO_2 adsorption selectivity and isosteric heats.

Conclusions

In summary, through successive functionalization of a T-shaped pyridine-dicarboxylate ligand with amide and N-oxide groups, we have synthesized two isoreticular MOFs. The ingenious modification of pyridine-N into N-oxide donor endows charge variation and bent-binding, offering "open donor sites" for preferential CO_2 interactions to remarkably enhance CO_2 adsorption enthalpy and separation selectivities over CH_4, CO and N_2 at room temperature. The mechanism of CO_2 adsorption and preferred binding sites have been studied and elucidated by theoretical simulations, which reveal that N-oxidization of N-donor ligand may be considered as a new potential way to

functionalize porous MOFs for CO_2 sequestration, comparable to approaches by introducing OMSs and exposed N sites. Further studies will be conducted by fitting N-oxide groups into more ligands to generate porous MOFs for high CO_2 uptake, and evaluate the separation behavior in more practical conditions with regard to water stability and moisture influence.

Notes and references

[a] MOE Laboratory of Bioinorganic and Synthetic Chemistry, Lehn Institute of Functional Materials, School of Chemistry and Chemical Engineering, Sun Yat-Sen University, Guangzhou 510275, China.
Fax: +86 02084115178; E-mail: cesscy@mail.sysu.edu.cnre.
[b] State Key Laboratory of Applied Organic Chemistry, Lanzhou University, Lanzhou 730000, China.

††Electronic Supplementary Information (ESI) available: Syntheses, characterization, sorption and simulation details, and crystallographic data (CIF). See DOI: 10.1039/c000000x/

1 (a) S. Chu, *Science,* 2009, **325**, 1599. (b) J. R. Li, Y. Ma, M. C. McCarthy, J. Sculley, J. Yu, H. K. Jeong, P. B. Balbuena, H. C. Zhou, *Coord. Chem. Rev.,* 2011, **255**, 1791.

2 N. Tippayawong, Thanompongchart P, *Energy,* 2010, **35**, 4531.

3 E. B. Le Bouhelec, P. Mougin, A. Barreau, R. Solimando, *Energy Fuels*, 2007, **21**, 2044.

4 A. Sayari, Y. Belmabkhout, R. Serna-Guerrero, *Chem. Eng. J.,* 2011, **171**, 760.

5 (a) L. J. Murray, M. Dinca, J. R. Long, *Chem. Soc. Rev.,* 2009, **38**, 1294. (b) A. U. Czaja, N. Trukhan, U. Muller, *Chem. Soc. Rev.,* 2009, **38**, 1284. (c) K. Sumida, D. L. Rogow, J. A. Mason, T. M. McDonald, E. D. Bloch, Z. R. Herm, T. H. Bae, J. R. Long, *Chem. Rev.,* 2012, **112**, 724. (d) S. Kitagawa, R. Matsuda, *Coord. Chem. Rev.,* 2007, **251**, 2490. (e) Z. J. Zhang, Y. G. Zhao, Q. H. Gong, Z. Li, J. Li, *Chem. Commun.*, 2013, **49**, 653. (f) J. Liu, P. K. Thallapally, B. P. McGrail, D. R. Brown, J. Liu, *Chem. Soc. Rev.,* 2012, **41**, 2308.

6 (a) M. Yoon, R. Srirambalaji, K. Kim, *Chem. Rev.,* 2012, **112**, 1196. (b) L. Q. Ma, C. Abney, W. B. Lin, *Chem. Soc. Rev.,* 2009, **38**, 1248. (c) J. Lee, O. K. Farha, J. Roberts, K. A. Scheidt, S. T. Nguyen, J. T. Hupp, *Chem. Soc. Rev.,* 2009, **38**, 1450. (d) Z. Wang, G. Chen, K. Ding, *Chem. Rev.* 2009, **109**, 322. (e) D. Farrusseng, S. Aguado, C. Pinel, *Angew. Chem., Int. Ed.* 2009, **48**, 7502.

7 (a) T. Devic, P. Horcajada, C. Serre, F. Salles, G. Maurin, B. Moulin, D. Heurtaux, G. Clet, A. Vimont, J.-M. Greneche, B. L. Ouay, F. Moreau, E. Magnier, Y. Filinchuk, J. Marrot, J.-C. Lavalley, M. Daturi, G. Ferey, *J. Am. Chem. Soc.,* 2010, **132**, 1127. (b) V. Colombo, C. Montoro, A. Maspero, G. Palmisano, N. Masciocchi, S. Galli, E. Barea, J. A. R. Navarro, *J. Am. Chem. Soc.,* 2012, **134**, 12830. (c) R. Vaidhyanathan, S. S. Iremonger, G. K. H. Shimizu, P. G. Boyd, S. Alavi, T. K. Woo, *Angew. Chem. Int. Ed,* 2012, **51**, 1826.

8 (a) J. B. Lin, J. P. Zhang, X. M. Chen, *J. Am. Chem. Soc.,* 2010, **132**, 6654. (b) P. Cui, Y. G. Ma, H. H. Li, B. Zhao, J. R. L, P. Cheng, P. B. Balbuena, H. C. Zhou, *J. Am. Chem. Soc,* 2012, **134**, 18892. (c) J. S. Qin, Du, Y. D. W. L. Li, J. P. Zhang, S. L. Li, Z. M. Su, X. L. Wang, Q. Xu, K. Z. Shao, Y. Q. Lan, *Chem. Sci,* 2012, **3**, 2114.

9 (a) J. Y. Lee, J. Li, J. Jagiello, *J. Solid State Chem.,* 2005, **178**, 2527. (b) C. Montoro, E. García, S. Calero, M. A. Pérez-Fernández, A. L. López, E. Barea, J. Navarro, *J. Mater. Chem.,* 2012, **22**, 10155. (c) Y. W. Li, J. R. Li, L. F. Wang, B. Y. Zhou, Q. Chen, X. H. Bu, *J. Mater. Chem., A*, 2013, **1**, 495.

10 (a) M. P. Cheon, E. Y. E. Suh, Y. Lee, *Chem. Eur. J.,* 2007, **13**, 4208. (b) C. L. Chen, A. M. Goforth, M. D. Smith, C.Y. Su, H. C. zurLoye, *Angew. Chem. Int. Ed.,* 2005, **44**, 6673.

11 a) S. L. Xiang, J. Huang, L. Li, J. Y. Zhang, L. Jiang, X. J. Kuang, C.-Y. Su, *Inorg. Chem., 2*011, **50**, 1743. (b) J. J. Jiang, R. Yang, Y. Xiong, L. Li, M. Pan, C.-Y. Su, *Sci. China Chem.,* 2011, **54**, 1436. (c) M. S. Chen, M. Chen, T.-A. Okamura, W. Y. Sun, N. Ueyama, *Microporous Mesoporous Mater,* 2011, **139**, 25. (d) X. F. Liu, M. Oh, M. S. Lah, *Inorg. Chem.,* 2011, **50**, 5044. (e) J. F. Eubank, L. Wojtas,

M. R. T. Hight, Bousquet, V. C. Kravtsov, M. Eddaoudi, *J. Am. Chem. Soc.,* 2011, **133**, 17532. (f) A. Schoedel, W. Boyette, L. Wojtas, M. Eddaoudi, M. J. Zaworotko, *J. Am. Chem. Soc., 2*013, **135**, 14016.

12 (a) C. Serre, S. Bourrelly, A. Vimont, N. A. Ramsahye, G. Maurin, P. L. Llewellyn, M. Daturi, Y. Filinchuk, O. Leynaud, P. Barnes, G. Férey, *Adv. Mater.* 2007, **19**, 2246. (b) P. K. Thallapally, J. Tian, M. R. Kishan, C. A. Fernandez, S. J. Dalgarno, P. B. McGrail, J. E. Warren, J. L. Atwood, G. *J. Am. Chem. Soc.* 2008, **130**, 16842. (c) Férey, C. Serre, *Chem. Soc. Rev.*, 2009, **38**, 1380.

13 (a) L. L. Wen, F. M. Wang, X. K. Leng, M. M. Wang, Q. J. Meng, H. Z. Zhu, *J. Inorg. Organomet. Polym., 2*010, **20**, 313. (b) L. Ducháčková, V. Steinmetz, J. Lemaire, J. Roithová, *Inorg. Chem.,* 2010, **49**, 8897. (c) E. Deiters, V. Bulach, M. Hosseini, W. *Dalton Trans., 2*007, 4126.

14 (a) Z. He, Z. M. Wang, C. H. Yan, *CrystEngComm.,* 2005, **7**, 143. (b) X. M. Zhang, Y. Q. Wang, X. B. Li, E. Q. Gao, *Dalton Trans.,* 2012, **41**, 2026.

15 (a) L. Qiu, J. G. Lin, Y. Y. Xu, *Inorg. Chem. Commun., 2*009, **12**, 986. (b) L. J. Zhang, D. H. Xu, Y. S. Zhou, F. Jiang, *New J. Chem, 2*010, **34**, 2470. (c) Y. Y. Xu, J. G. Lin, J. Yao, S. Gao, H. Z. Zhu, Q. J. Meng, *Inorg. Chem. Commun., 2*008, **11**, 1422.

16 (a) J. Sun, Y. Zhou, Q. Fang, Z. Chen, L. Weng, G. Zhu, S. Qiu, D. Zhao, *Inorg. Chem.,* 2006, **45**, 8677. (b) G. H. Xu, X. G. Guo, P. Zhang, C. L. Pan, H. J. Zhang, C. Wang, *J. Am. Chem. Soc., 2*010, **132**, 3656. (c) X. M. Lin, T. T. Li, L. F. Chen, L. Zhang, C. Y. Su, *Dalton Trans., 2*012, **41**, 10422.

17 (a) V. Blatov, A. *IUCr Comp. Comm. Newslett., 2*006, **7**, 4. (b) V. A. Blatova, D. M. Proserpio, *ActaCrystallogr, 2*009, **A65,** 202.

18 A. Spek, *J. Appl. Crystallogr.,* 2003, **36**, 7.

19 J. An, S. J. Geib, N. L. Rosi, *J. Am. Chem. Soc, 2*010, **132**, 38.

20 (a) A. L. Myers, J. M. Prausnitz, *J. AIChE* 1965, **11**, 121. (b) L. J. Y. S. Bae, K. L. Mulfort, H. Frost, P. Ryan, S. Punnathanam, Broadbelt, J. T. Hupp, R. Q.Snurr, *Langmuir,* 2008, **24**, 8592.

21 J. M. Simmons, H. Wu, W. Zhou, T.Yildirim, *Energy Environ. Sci.,* 2011, **4**, 2177.

22 (a) P. S. Nugent, V. L. Rhodus, T. Pham, K. Forrest, L. Wojtas, B. Space, M. J. Zaworotko, *J. Am. Chem. Soc.* 2013, **135**, 10950. (b) W. M. Bloch, R. Babarao, M. R. Hill, C. J. Doonan, C. J. Sumby, *J. Am. Chem. Soc.* 2013, **135**, 10441. (c)) P. Nugent, Y. Belmabkhout, S. D. Burd, A. J. Cairns, R. Luebke, K. Forrest, T. Pham, S. Ma, B. Space, L. Wojtas, M. Eddaoudi, M. J. Zaworotko, *Nature,* 2013, **495**, 80.

23 (a) D. Saha, Z. B. Bao, F. Jia, S. G. Deng, *Environ. Sci. Technol.*, 2010, **44***,* 1820. (b) R. Banerjee, H. Furukawa, D. Britt, C. Knobler, M. O'Keeffe, O. M. Yaghi, *J. Am. Chem. Soc.,* 2009, **131**, 3875. (c) A. Demessence, D. M. D'Alessandro, M. L. Foo, J. R. Long, *J. Am. Chem. Soc.,* 2009, **131**, 8784.

24 J. McEwen J. D. Hayman, O.Yazaydin, *Chem. Phys.,* 2013, **412**, 72.

25 (a) T. M. McDonald, D. M. D'Alessandro, R. Krishna, J. R. Long, *Chem. Sci.,* 2011, **2**, 2022. (b) P. Aprea, D. Caputo, N. Gargiulo, F. Iucolano, F. J. Pepe, *Chem. Eng. Data,* 2010, **55**, 3655. (c) T. M. McDonald, W. R. Lee, J. A. Mason, B. M. Wiers, C. S. Hong, J. R. Long, *J. Am. Chem. Soc., 2*012, **134**, 7056. (d) L. Du, Z. Lu, K. Zheng, J. Wang, X. Zheng, Y. Pan, X. You, J. Bai, *J. Am. Chem. Soc, 2*012, **135**, 562.

26 J. L. C. Rowsell, O. M. Yaghi, *J. Am. Chem. Soc.,* 2006, **128**, 1304.

27 J. M. Gu, T. H. Kwon, J. H. Park, S. Huh, *Dalton Trans,* 2010, **39**, 5608.

28 S. Kirkpatrick, C. D. Gelatt, M. P. Vecchi, *Science,*1983, **220**, 671.